

Technical University of Denmark



## The Solent sonic - response and associated errors

**Mortensen, Niels Gylling; Højstrup, J.**

*Published in:*

Ninth symposium on meteorological observations and instrumentation. Preprints

*Publication date:*

1995

*Document Version*

Publisher's PDF, also known as Version of record

[Link back to DTU Orbit](#)

*Citation (APA):*

Mortensen, N. G., & Højstrup, J. (1995). The Solent sonic - response and associated errors. In Ninth symposium on meteorological observations and instrumentation. Preprints (pp. 501-506). Boston, MA: American Meteorological Society.

## DTU Library

Technical Information Center of Denmark

---

### General rights

Copyright and moral rights for the publications made accessible in the public portal are retained by the authors and/or other copyright owners and it is a condition of accessing publications that users recognise and abide by the legal requirements associated with these rights.

- Users may download and print one copy of any publication from the public portal for the purpose of private study or research.
- You may not further distribute the material or use it for any profit-making activity or commercial gain
- You may freely distribute the URL identifying the publication in the public portal

If you believe that this document breaches copyright please contact us providing details, and we will remove access to the work immediately and investigate your claim.

Niels G. Mortensen and Jørgen Højstrup\*

Risø National Laboratory  
Roskilde, Denmark

## 1 INTRODUCTION

Sonic anemometers can provide in-situ measurements of the wind velocity components and the temperature, with high temporal and spatial resolution. From these measurements the mean wind speeds and temperature, as well as the turbulence intensities, shear stresses, heat flux, atmospheric stability etc. can be derived. Since sonics have no moving parts they have none of the response problems associated with mechanical anemometers, and for the same reason they presumably require very little maintenance. A sonic anemometer therefore seems to be the instrument of choice for many applications within the atmospheric boundary layer where long-term, accurate measurements of the turbulent characteristics of the atmosphere are wanted.

However, sonic anemometers also have a number of less favourable characteristics, the most important being the distortion of the flow by the probe head itself. Whereas instrument cost and ease-of-operation in the field are probably of less concern now, the determination of the flow distortion and other response characteristics unfortunately still requires fairly comprehensive investigations by the sonic manufacturer and/or user. Despite efforts in design and testing, sonic response characteristics and the associated errors are therefore often not known or documented in detail.

Field intercomparison studies provide a means of assessing the overall accuracy of sonic measurements. Recently, the Atmospheric Technology Division of NCAR conducted such an experiment, inter-comparing three state-of-the-art sonic anemometers and a propeller anemometer. The experiment was carried out under nearly ideal experimental conditions and subsequent analyses were limited to wind directions where the measurements would be least influenced by terrain inhomogeneities or flow distortion by the masts and other experimental equipment. The results showed systematic differences between different sonics—typically 5% in mean wind speed ( $U$ ), 10–15% in friction velocity ( $u_*$ ), 10% in the standard deviations of the longitudinal and transversal wind speed components ( $\sigma_u$  and  $\sigma_v$ ), and

10–15% in the standard deviations of the vertical wind speed component ( $\sigma_w$ ) and the absolute temperature ( $\sigma_T$ ). Two of the sonics employed were a Solent research model (1012/R2) and a Kaijo Denki A-probe (TR-61A). Some results of the intercomparison for these two sonics are given in Tab. 1.

Table 1: Comparison of mean wind speeds, friction velocities, and standard deviations of wind speeds and temperature measured with a propeller and two sonic anemometers.  $a$  and  $b$  are the coefficients of a linear fit to the data:  $Y = aX + b$ .

	$X$	$Y$	$a$	$b$
$\bar{U}$	Propeller	Solent	0.962	0.057
$u_*$	Kaijo Denki	Solent	0.870	0.009
$\sigma_u$	Kaijo Denki	Solent	0.946	0.011
$\sigma_v$	Kaijo Denki	Solent	0.893	0.018
$\sigma_w$	Kaijo Denki	Solent	0.884	0.009
$\sigma_T$	Kaijo Denki	Solent	0.864	0.067

The intercomparison suggests that the Solent sonic may be underestimating the wind speed components and the temperature variance. These and other field observations have led us to take a closer look at Solent sonic response characteristics and associated errors. The following is a preliminary report of our findings.

## 2 THE SOLENT SONIC ANEMOMETER

The three-dimensional sonic system described below is the Solent 1012 research model with an omnidirectional sensor array, manufactured by Gill Instruments Ltd. The sonic array has three intersecting paths oriented at 120° azimuth intervals and at an inclination from the vertical of 45°, see Fig. 1. The top and bottom of the array are connected by three struts ( $\emptyset = 6.2$  mm) at 120° azimuth intervals, offset by 30° to the path azimuths. The array is mounted on the top of a tube extending 500 mm below the array. The path length is 149 mm and the transducer diameter 12 mm, which gives a path-length to transducer-diameter ratio approx. equal to 12.

The Solent probe heads are manufactured in two different configurations: an omnidirectional and an asymmetric type; here we will focus on the omnidirectional type. The electronics is housed in the lower

\* *Corresponding author address:* Niels G. Mortensen, Department of Meteorology and Wind Energy, Risø National Laboratory, P.O. Box 49, DK-4000 Roskilde, Denmark.

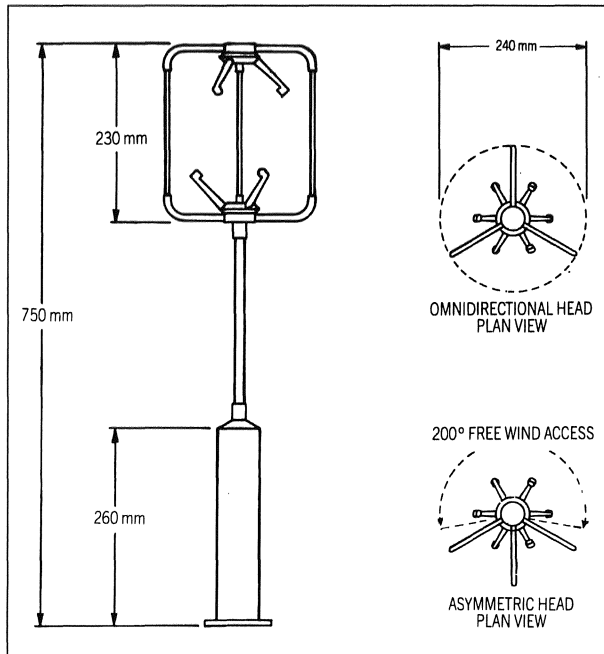


Figure 1: The Solent 1012 sonic anemometer/thermometer (Gill Instruments, 1990). The strut pointing upwards in the plan view for the omnidirectional head is taken as  $0^\circ$  (N) below.

large-diameter tube and each research model comes with an instrument-specific calibration table for on-line correction of the horizontal response. This table was obtained by the manufacturer by measuring the horizontal wind speed and direction in a wind tunnel. Generic calibration tables for the vertical response are also included (Gill Instruments, 1990).

### 3 SOLENT RESPONSE CHARACTERISTICS

The flow response and other characteristics of the sonic were investigated in our workshop, in an environmental chamber and in a wind tunnel.

The low-speed ( $0\text{--}10\text{ ms}^{-1}$ ) wind tunnel has a cross-section of  $1.75\text{ m} \times 1.55\text{ m}$  ( $w \times h$ ). The mean speed has been found to vary  $\pm 1\%$  in the measuring cross section (S.O. Hansen, pers. comm.) and turbulence levels are 2–3%. Flow speeds of 3, 6 and  $9\text{ ms}^{-1}$  were used, but the measurements reported here were mostly obtained at  $6\text{ ms}^{-1}$ . The reference speed in the tunnel was measured with a pitot-static tube and a precision pressure transducer.

#### 3.1 Sonic probe geometry

The array geometry enters in the transformation of the wind speed components, measured along the sound paths, into the Cartesian components of a conventional  $(u, v, w)$  coordinate system. Using the nominal values of the probe angles and path lengths,

inaccuracies in the manufacturing of the probe head thus translate into errors in the transformed wind components.

The geometry of several Solent sonic probes were measured in a jig boring machine in the Risø workshop, see Tab. 2. Here, the inclination of the sound paths is determined with respect to the plane defined by the bottom triangle of transducers. Repeated measurements on the same probe indicate that the accuracy is about  $0.1^\circ$  for angle and 0.1 mm for length determinations, respectively.

Table 2: Deviations in angles and path lengths from the nominal and mean values, respectively, for two omnidirectional (O) and two asymmetric probe heads (A).

Solent	Vertical	Horizontal	Path length
#0017 (O)	$0.68^\circ$	$-2.74^\circ$	$-0.31\text{ mm}$
	$0.69^\circ$	$-2.01^\circ$	$0.06\text{ mm}$
	$0.54^\circ$	$-2.08^\circ$	$0.26\text{ mm}$
#0028 (O)	$0.29^\circ$	$-1.63^\circ$	$0.98\text{ mm}$
	$1.04^\circ$	$-0.78^\circ$	$-0.19\text{ mm}$
	$0.59^\circ$	$-1.13^\circ$	$-0.80\text{ mm}$
#0032 (A)	$2.05^\circ$	$-1.16^\circ$	$-1.20\text{ mm}$
	$0.31^\circ$	$-0.03^\circ$	$1.32\text{ mm}$
	$0.75^\circ$	$-1.70^\circ$	$-0.12\text{ mm}$
#0033 (A)	$1.97^\circ$	$-0.45^\circ$	$-0.33\text{ mm}$
	$0.82^\circ$	$0.93^\circ$	$0.69\text{ mm}$
	$1.09^\circ$	$-0.07^\circ$	$-0.36\text{ mm}$

The transformation errors in the horizontal wind speed components are likely to be negligible and further, they are compensated for when applying the built-in calibration tables for  $u$  and  $v$ . However, the vertical component—and higher order statistics—may suffer more severely and this is not compensated for by the manufacturers correction procedure. These and other alignment errors may be alleviated if the turbulence statistics are transformed into a coordinate system aligned with the mean flow. Here we have used the measured probe angles and path lengths in the calculation of the tunnel-derived wind components and transducer delays.

#### 3.2 Temperature sensitivity of transducers

Wind speeds measured by sonics are in principle independent of pressure, air temperature, humidity etc. However, temperature variations may cause small variations in the properties of transducers (K. Lawes, pers. comm.) and electronics, whereby the measured flight time of the sound pulse becomes a function of not only the flow speed, but also of the ambient temperature.

This effect was assessed by mounting the sonic probe head and electronics in an environmental chamber at zero wind speed. Flight time measure-

ments were taken in both directions at 10-degree intervals over the range of  $-10^{\circ}$  to  $30^{\circ}\text{C}$ . The results for Solent #28 are given in Fig. 2.

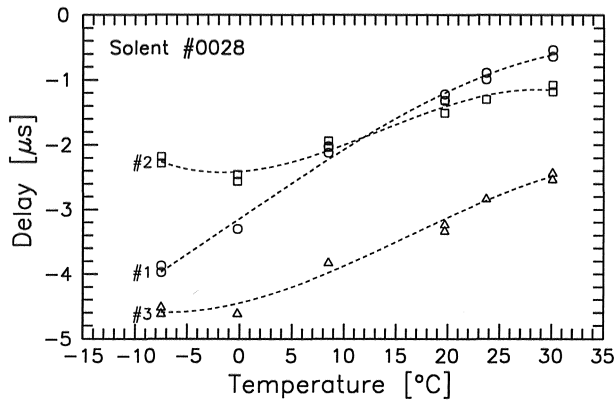


Figure 2: Temperature sensitivity of the flight-time measurements along the three paths of Solent sonic #28. Dashed lines are polynomial fits to the data. A typical flight time is  $450\ \mu\text{s}$  at  $0^{\circ}\text{C}$ .

The delay was calculated as the difference between the flight time measured by the sonic and the flight time inferred from the temperature of the chamber and the (measured) length of the sound path. For each sound path at one temperature two delays are shown, corresponding to sound pulses traveling in opposite directions along the path. Figure 2 shows that there are clear variations in delay versus temperature along each of the three paths and also that the two delays for each path are practically the same.

This temperature sensitivity affects both the wind speed and temperature output of the sonic: the maximum errors in horizontal wind speed and absolute temperature over the range of  $-10^{\circ}$  to  $+30^{\circ}\text{C}$ , corresponding to the delay variations depicted in Fig. 2, are 2% and 5K, respectively. In the interval from  $5^{\circ}$  to  $35^{\circ}\text{C}$  the errors are within the accuracy specified by the manufacturer (Gill Instruments, 1990). Once the delay variations have been determined, these can of course be programmed into the anemometer or data analysis software.

### 3.3 Transducer shadow effect

One of the well-known errors in sonic anemometry is the transducer shadow effect, i.e. the underestimation of the wind components measured along the acoustic paths due to velocity deficits in the wakes of the transducers (Kaimal, 1979). This effect was not specifically investigated and so far no parameterization seems to have been published for Solent type transducers. However, since the sound paths are inclined  $45^{\circ}$  to the horizontal this effect is presumably small in most applications (Mortensen, 1994). Here, it will be treated as part of the array flow distortion.

### 3.4 Array flow distortion—horizontal flow

To investigate the flow distortion by the entire sonic array, the probe was exposed to a laminar wind-tunnel flow and systematically rotated  $360^{\circ}$  in the horizontal and through the range of  $+20^{\circ}$  to  $-20^{\circ}$  in the vertical. The increment in azimuth was  $5^{\circ}$  for both horizontal and inclined flow, i.e. with the probe tilted  $\pm 1^{\circ}$ ,  $\pm 3^{\circ}$ ,  $\pm 5^{\circ}$ ,  $\pm 10^{\circ}$ ,  $\pm 15^{\circ}$  and  $\pm 20^{\circ}$ . In each position measurements were averaged over 20 seconds. The measured flow distortion for horizontal flow by Solent #28 is shown in Fig. 3.

The speed ratio is defined here as  $U_{\text{sonic}}/U_{\text{pitot}}$ , where  $U_{\text{sonic}}$  is calculated from the uncorrected sonic speeds. The flow angle-of-attack in the horizontal is calculated from the turn-table azimuth and given as a wind direction—using the standard meteorological convention. North ( $0^{\circ}$ ) corresponds to one of the struts connecting the lower and upper part of the anemometer, see Fig. 1.

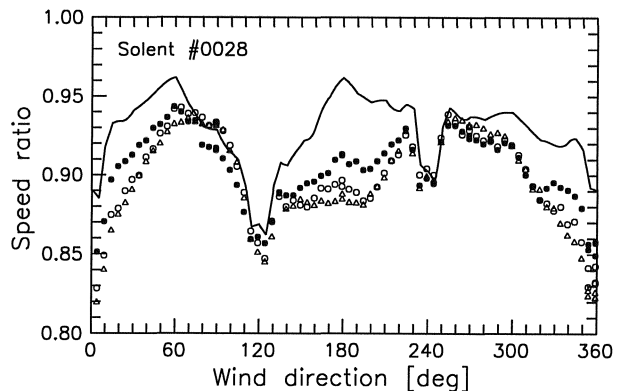


Figure 3: The sonic response to a horizontal flow of  $6\ \text{ms}^{-1}$  for different azimuth angles in a wind tunnel. The increment in azimuth is  $5^{\circ}$  and three different runs are shown. The corresponding curve derived from the manufacturer's correction tables are shown with a full line.

Overall, the sonic array seems to reduce the flow speed by about 10%. Furthermore, the sonic response varies systematically by more than 10% with wind direction: the supporting struts reduce the wind speed considerably, whereas the speed ratios show (weak) local maxima when the flow is directed unobstructed towards the transducers. This behaviour, as well as the magnitude of the distortion, is comparable to that of the Kaijo Denki TR-61B probe which has the same basic geometry as the Solent (Mortensen, 1994).

Each Solent research model sonic comes with instrument-specific calibration tables for on-line correction of the horizontal wind speeds. The corresponding correction curve for Solent #28 is shown with a full line in Fig. 3 and was determined by the manufacturer in a wind tunnel at  $20\ \text{ms}^{-1}$  (Gill

Instruments, 1990). Obviously, the two independent determinations agree only partly, the difference being almost 10% for some directions.

The array flow distortion changes not only the magnitude of the wind vector, but also its angle-of-attack in the horizontal (wind direction) and vertical (pitch). Pitch errors are particularly important since they show up as apparent vertical wind speeds. The measured pitch of the wind vector for horizontal flow is shown in Fig. 4.

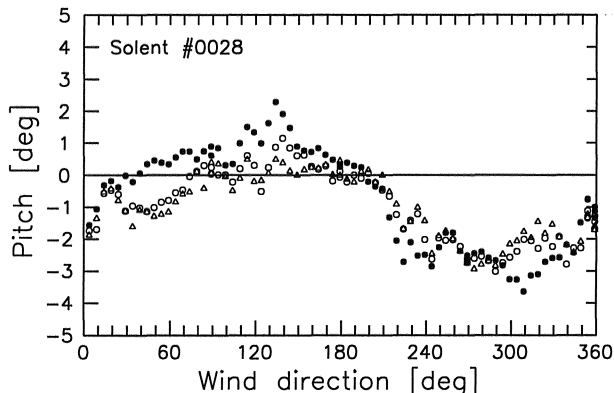


Figure 4: Pitch of the wind vector for horizontal flow in a wind tunnel. The increment in azimuth is  $5^\circ$  and data from three different runs are shown.

The pitch error can be largely described as a  $360^\circ$ -modulation with an amplitude of more than  $1.5^\circ$  and an offset of almost  $-1^\circ$ . There are several reasons for this variation: Firstly, the actual probe geometry gives rise to an apparent pitch because the transformations of wind speeds are calculated using the nominal geometry. Secondly, the probe was aligned in the wind tunnel by adjusting the turntable to a position where the vertical axis of the instrument (ie the tube below the array) was perpendicular to the tunnel wall. Later measurements have shown that the plane described by the three bottom transducers is not perpendicular to this axis. Finally, other investigations in the same wind tunnel seem to indicate that the flow in the working section may not be entirely parallel to the tunnel walls (L. Kristensen, pers. comm.).

### 3.5 Sensitivity to flow speed

The flow distortion by some sonic probes—or part of the distortion—has been shown to depend on flow speed (see e.g. Mortensen [1994]). Within the limited range of wind speeds used in this study, no dependence on flow speed was observed.

### 3.6 Array flow distortion—inclined flow

Non-horizontal flow was simulated in the wind tunnel by tilting the sonic probe  $\pm 1^\circ$ ,  $\pm 3^\circ$ ,  $\pm 5^\circ$ ,  $\pm 10^\circ$ ,

$\pm 15^\circ$  and  $\pm 20^\circ$  relative to its vertical axis. The comparison between the sonic-measured and tunnel-derived vertical wind speeds is shown in Fig. 5.

Here we compare the *calibrated* vertical component from the sonic, calculated using the calibration tables supplied by the manufacturer. The mean pitch measured for horizontal flow has been taken into account, i.e. the comparison is forced through  $(0, 0)$ . The overall comparison (marked with  $\times$ 's) indicates that the calibrated sonic speeds are approx. 7% lower than the tunnel-derived speeds. The scatter around this value is resolved when we compare vertical wind speeds for each wind direction. In Fig. 5 are also shown the comparisons at wind directions of  $0^\circ$ ,  $90^\circ$ ,  $180^\circ$  and  $270^\circ$ , where additional measurements for every  $1^\circ$  change of inclination were made. For each of these directions we thus have more than fifty 20-second measurements. The relations between vertical wind speeds for these (and other) directions are remarkably linear (cf. Mortensen, 1994), though not always with a 1:1 slope.

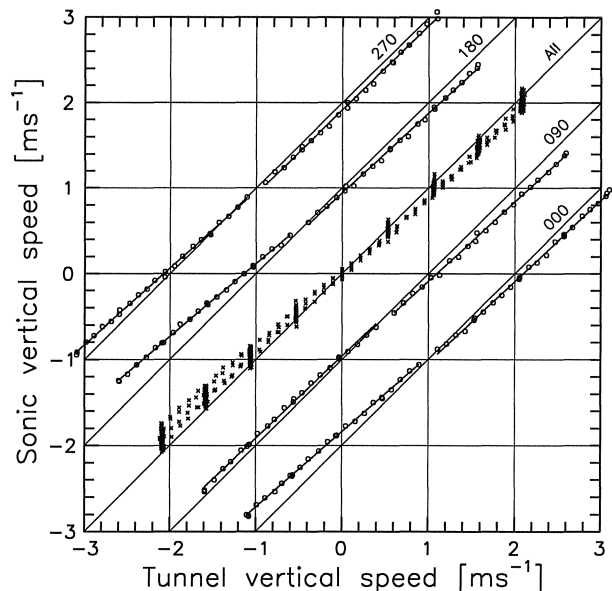


Figure 5: Comparison of Solent calibrated vertical wind speeds and vertical wind speeds derived from the wind tunnel. The overall comparison between  $w_s$  and  $w_t$  is shown with  $\times$  symbols. For display purposes, the data points have been displaced  $\pm 0.5$  and  $\pm 1.0 \text{ ms}^{-1}$  for the comparisons at wind directions of  $0^\circ$ ,  $90^\circ$ ,  $180^\circ$  and  $270^\circ$ .

In a similar manner straight lines can be fitted to points comparing tunnel-derived with *un-calibrated* Solent vertical speeds. This has been done for 72 equidistantly separated wind directions to calculate the vertical response as the speed ratio  $w_{\text{sonic}}/w_{\text{tunnel}}$ . The variation of this ratio with wind direction is shown in Figs. 6 and 7 for positive (upwards) and negative (downwards) vertical wind

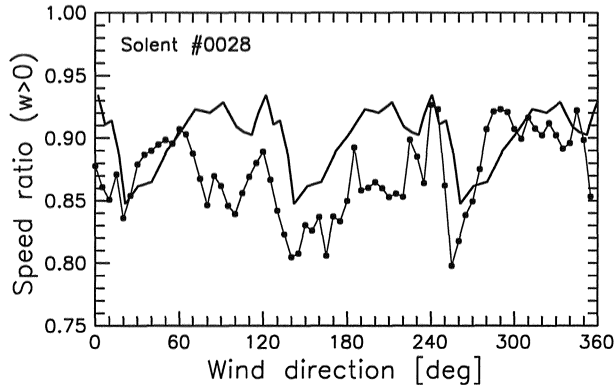


Figure 6: Ratios of un-calibrated sonic vertical wind speeds to tunnel-derived vertical wind speeds (dots) as a function of wind direction—for positive speeds. Manufacturer's generic calibration table is shown with a thick full line.

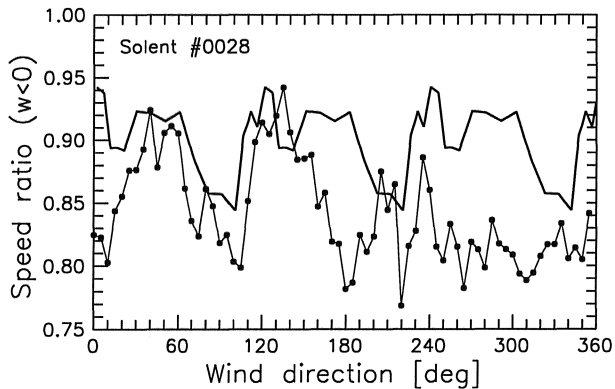


Figure 7: Same as Fig. 6, but for negative (downwards) vertical wind speeds.

speeds, respectively. Also shown are the corresponding curves calculated from the generic  $w$ -calibration tables supplied by the manufacturer. As might be expected, the generic calibration curves do not describe the measured response of Solent #28 in detail and fairly large (azimuth-dependent) differences are observed.

#### 4 SOLENT TEMPERATURES

The Solent sonic also provides a speed-of-sound output calculated from the transit times along the  $T_1$  path, i.e. the path with orientation  $330^\circ$ – $150^\circ$  (Gill Instruments, 1990). The sonic temperature was calculated from the speed of sound as described by e.g. Kaimal and Gaynor (1991), including correction for the cross-wind contamination of the temperature. The comparison between tunnel temperature measured with a pt-100 temperature sensor and sonic temperature is shown in Fig. 8.

Within the limited range of temperatures ob-

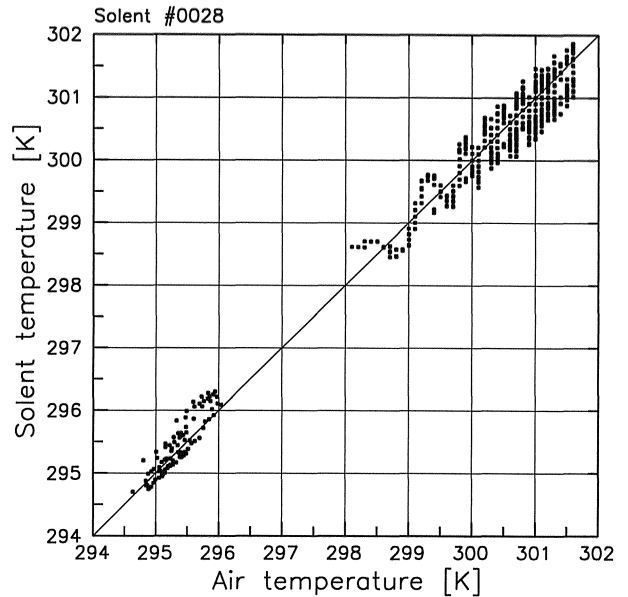


Figure 8: Comparison of air temperature measured in the wind tunnel and Solent sound-virtual temperature.

served the comparison of sonic and tunnel temperature is practically linear and along the 1:1-line. However, the measurements show considerable scatter. The origin of this is in the sonic temperature, which varies by about  $\pm 0.5$  K depending on wind direction. The reason for this unexpected behaviour is not yet known.

#### 5 DISCUSSION

The comparisons of wind speeds measured by Solent #28 and wind speeds derived from the wind tunnel are summarized in Tab. 3. Both the horizontal and vertical response improve significantly when employing the instrument-specific and generic correction tables supplied by the manufacturer. Using the calibrated outputs, the wind speed components still seem to be underestimated by the Solent—somewhat less, however, than was found in the field intercomparison. In a wind tunnel study of an asymmetric probe head, Kunz (1994) found that the horizontal sonic wind speed was about 4.5% higher than the reference speed in the wind tunnel.

It should be borne in mind though, when evaluating the absolute accuracy of the sonic, that the reference speed in our wind tunnel tests could also be questioned. Firstly, the wind speed in the tunnel has been reported to vary  $\pm 1\%$  in the working cross section. Secondly, the size of the wind tunnel facility made it difficult to keep the room temperature constant, and this might affect the accuracy of the reference speed measurement. This effect was estimated by varying the temperature of the pres-

sure transducer and other equipment in an environmental chamber, while keeping the temperature of the wind tunnel constant. In this way, the reference speed was indeed found to vary with temperature, by about 0.3% per degree in the temperature interval reported here. This variation has been taken into account in all of the data shown above, where the speeds derived from the pitot-static tube have been referenced to 15°C—close to the temperature at which the manometer was calibrated.

Table 3: Comparison of mean wind speeds derived from the wind tunnel and measured by Solent #28. Speeds calculated using the correction tables supplied by the manufacturer are denoted “Solent cal.”.  $S_1$ ,  $S_2$  and  $S_3$  are the components along each path and  $a$  and  $b$  are the coefficients of a linear fit to the data (1025 observations):  $Y = aX + b$ .

	$X$	$Y$	$a$	$b$
$U$	tunnel	Solent raw	0.899	—
	tunnel	Solent cal.	0.969	—
$u$	tunnel	Solent raw	0.921	-0.007
	tunnel	Solent cal.	0.993	-0.017
$v$	tunnel	Solent raw	0.877	0.080
	tunnel	Solent cal.	0.945	0.065
$w$	tunnel	Solent raw	0.836	0.016
	tunnel	Solent cal.	0.928	0.018
$S_1$	tunnel	Solent raw	0.896	0.001
	tunnel	Solent cal.	0.955	-0.057
$S_2$	tunnel	Solent raw	0.907	0.056
	tunnel	Solent cal.	1.004	-0.002
$S_3$	tunnel	Solent raw	0.905	0.101
	tunnel	Solent cal.	0.966	0.023

Whereas the absolute accuracy may not be a cause for concern, the azimuth-dependent variations of the wind speed and temperature outputs should be. In Section 3 we reported azimuth-dependent variations of the vertical response that were not taken into account by the generic correction tables. Furthermore, the temperature output was found to vary with azimuth, even though we do not understand the reason for this. Finally, the differences between the correction tables determined by the manufacturer for horizontal flow and the speed ratios obtained here (Fig. 3) are also seen to depend on wind direction. This is further illustrated in Fig. 9, where ratios of calibrated sonic wind speeds and wind tunnel speeds in two runs are plotted as a function of wind direction.

In addition to a pronounced variation of the speed ratios with wind direction, the two runs also show that this speed ratio may depend on other characteristics of the run, possibly temperature. The reason for this is not yet known.

The results reported here should be considered preliminary since we have not been able to account

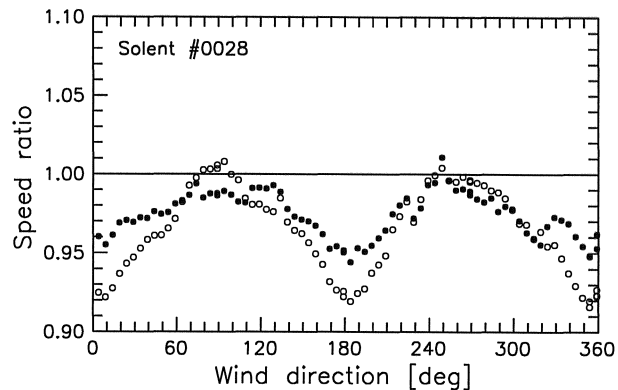


Figure 9: Ratios of calibrated (manufacturers calibration) horizontal wind speed and wind tunnel speed as a function of wind direction for Solent sonic #28. Tunnel speed in both runs was  $6.1 \text{ ms}^{-1}$ , mean tunnel temperature was  $25.8^\circ\text{C}$  (●) and  $28.4^\circ\text{C}$  (○), respectively.

for certain characteristics of the sonic response. When these have been analyzed in more detail, a correction procedure for the Solent can be established and the errors in turbulence statistics measured with this probe evaluated.

#### ACKNOWLEDGEMENTS

The sonic field comparison data were collected by the Atmospheric Technology Division of the National Center for Atmospheric Research (NCAR) during the STORM-FEST experiment in 1992.

The analyses presented here were initiated while the authors were visiting scientists at NCAR. Discussions with T. Horst and S. Oncley of the Atmospheric Technology Division are gratefully acknowledged.

Thanks are finally due to L. Kristensen, Risø, for many valuable comments on a draft of this paper.

#### REFERENCES

- Gill Instruments (1990). Gill Instruments 3-axis research ultrasonic anemometer. Product specification 4.0. Gill Instruments Ltd, Lymington, 45 p.
- Kaimal, J.C. (1979). Sonic anemometer measurement of atmospheric turbulence. *Proc. Dynamic Flow Conference*, Skovlunde, Denmark, 551–565.
- Kaimal, J.C. and J.E. Gaynor (1991). Another look at sonic thermometry. *Boundary-Layer Meteorol.* **56**, 401–410.
- Kunz, G.J. (1994). Tests of a Gill ultrasonic anemometer (Solent) in a wind tunnel. TNO-report FEL-94-A118. 24 p.
- Mortensen, N.G. (1994). Flow-response characteristics of the Kaijo Denki omni-directional sonic anemometer (TR-61B). Risø-R-704(EN). 32 p.